JOURNAL OF APPLIED POLYMER SCIENCE VOL. 13, PP. 2297–2311 (1969)

Load–Compression Behavior of Flexible Foams

K. C. RUSCH, *Scientific Research Staff, Ford Motor Co., Dearborn, Michigan 48121*

Synopsis

The load–compression behavior of a foam reflects its geometric structure and the physical properties of the matrix polymer. Quantitative relations between these parameters have been established in the present study. Based on both theoretical analyses and experimental data obtained on a flexible polyurethane foam, it is shown that the compressive stress can be factored into the product of two terms: (1) a dimensionless function of the compressive strain, $\psi(\epsilon)$, calculated from experimental load–compression data and reflecting the buckling of the foam matrix; and (2) a factor, ϵE_f, where E_f is the apparent Young's modulus of the foam (which is a function primarily of the modulus of the base polymer E_0 and of the volume fraction of polymer, φ). Thus the compressive stress behavior of a foamed polymer is determined by E_0, φ, and the matrix geometry, the latter described by the function $\psi(\epsilon)$. Using these established relations, it now is possible to delineate precisely the structural features a foam must possess—density, cell shape and size distribution, and modulus of the base polymer—to meet a given load–compression specification.

INTRODUCTION

Although foamed polymers are used extensively for cushioning, load distribution, and energy absorption, little attention has been given to the influence of the geometric structure of the foam matrix on the load–compression behavior. A typical load–deflection curve for a low-density flexible foam, under uniaxial compression and tension, is shown in Figure 1. In extension the curve is linear up to approximately 10% elongation, but in compression the curve becomes decidedly nonlinear after only a few per cent deformation. The load–compression relation is typical of that for a buckling process and varies markedly between foams of different matrix geometry (Fig. 2). For energy absorption applications, a load–compression curve with a broad plateau (sample L or Q) is preferable since the maximum energy-absorbing efficiency is obtained from a material that compresses at constant stress. On the other hand, for applications such as cushioning or load distribution, a more linear load–compression curve (sample R or E) is desired.

To understand the relationship between the load–compression behavior and the physical properties and geometric structure of the matrix polymer, the compressive stress has been factored into the product of two terms: one dependent on the apparent Young's modulus of the foam and the other

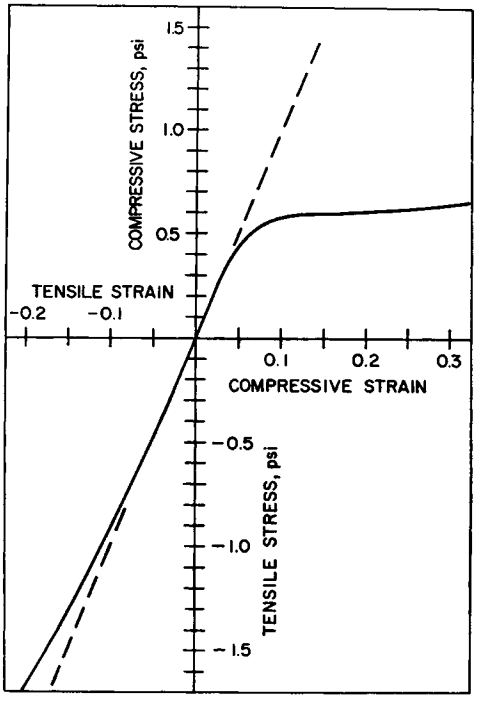

Fig. 1. Typical stress–strain curve for a low-density, flexible foamed polymer.

dependent on the geometric structure of the foam matrix. This procedure permits comparison of the influences of matrix geometry between foams of widely different stiffness.

The contribution of matrix geometry to the compressive stress, expressed as a dimensionless function of compressive strain, $\psi(\epsilon)$, is calculated from experimental load–compression curves for a series of low-density, flexible polyurethane foams of varying cell size, cell structure, and density. The function $\psi(\epsilon)$ is shown to vary in a regular manner with the geometric structure of the matrix.

ANALYTICAL APPROACH

The nonlinear character of the load–compression curves presumably arises solely from collapsing, or buckling, of the foam matrix, and it is appropriate to separate the compressive stress into a factor reflecting the apparent Young's modulus of the foam, E_f, and a factor reflecting the collapse of the matrix, $\psi(\epsilon)$. This can be expressed as follows:

$$\sigma = E_f \epsilon \psi(\epsilon) \tag{1}$$

where σ and ϵ are the compressive stress and strain, respectively, and E_f is the slope of the linear portion of the load–deformation curve; thus $\psi(\epsilon)$ approaches unity as ϵ approaches zero. This type of analysis has been

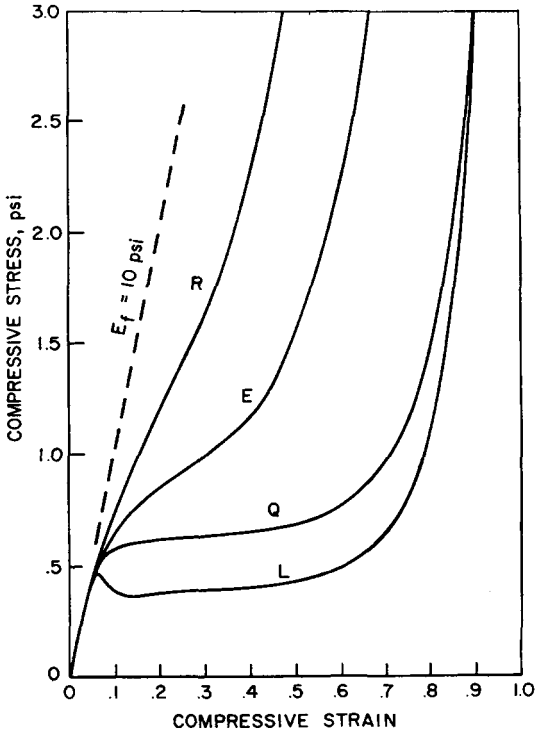

Fig. 2. Reduced compressive stress–strain curves for low-density, flexible foams of different cell geometry.

employed in the interpretation of other nonlinear systems[1,2] but has not been applied previously to compression of a foam.

In principle, $\psi(\epsilon)$ is dependent only on the geometric features of the matrix and independent of the modulus of the pure matrix polymer, E_0; therefore the time and temperature dependences characteristic of E_0 should influence E_f only.

The apparent modulus, E_f, also is dependent on matrix geometry, but in a different manner than $\psi(\epsilon)$. It has been shown both experimentally and theoretically[3–8] that the ratio E_f/E_0 depends primarily on the volume fraction of polymer, φ, and is largely independent of cell size. The following empirical equation[8] gives approximately the correct dependence for all values of φ if the cell geometry is close to spherical:

$$E_f/E_0 = \varphi(2 + 7\varphi + 3\varphi^2)/12. \tag{2}$$

This relationship between E_f/E_0 and φ has an initial slope of $1/6$, as predicted by Gent and Thomas,[3] and approaches unity as $\varphi \rightarrow 1$.

The shape of the load–compression curve varies markedly between foams of different cell geometry. Typical compression data for three polyurethane foams and a rubber latex foam are shown in Figure 2; the physical

TABLE I
Foam Characteristics

Sample	Foam type	E_f, psi	φ	Cell size, in. av.	Cell size, in. 95% range
A	polyurethane (I)	115.	0.34	0.005	0.0005–0.015
B	"	77.	0.24	0.007	0.001 –0.02
C	"	25.	0.11	0.012	0.003 –0.03
D	"	11.5	0.065	0.020	0.007 –0.05
E	"	4.5	0.043	0.022	0.008 –0.06
F	"	3.5	0.037	0.025	0.01 –0.06
G	polyurethane (II)	15.	0.033	0.020	0.01 –0.04
H	"	9.0	0.028	0.013	0.005 –0.025
J	"	14.	0.063	0.020	0.01 –0.04
K	"	32.	0.105	0.020	0.01 –0.04
L	reticulated polyurethane (II)	18.	0.028	0.10	0.04 –0.2
M	"	14.	0.028	0.050	0.02 –0.1
N	"	9.4	0.028	0.035	0.01 –0.08
P	"	16	0.028	0.020	0.01 –0.04
Q	"	11.	0.032	0.012	0.005 –0.02
R	rubber latex	4.9	0.12	0.010	0.001 –0.03

characteristics of these foams are listed in Table I. To permit an easy comparison, the compressive stress data in Figure 2 are reduced by a constant factor such that the initial slope corresponds to an E_f of 10 psi for each curve. The same reduced compression curves are plotted on logarithmic coordinates in Figure 3 and the $\psi(\epsilon)$ functions are shown in Figure 4. Equation (1) is employed to compute $\psi(\epsilon)$ from σ as a function of ϵ, after E_f has been evaluated from tensile stress–strain data or from compression data at small strains.

The log $\psi(\epsilon)$–log ϵ curve has several distinct features, corresponding to features of the load–compression curve, which are readily seen by comparing Figure 4 to Figures 2 and 3. Below some critical strain, the load–compression curve is linear and $\psi(\epsilon) = 1.0$. Then, as the matrix begins to buckle, $\psi(\epsilon)$ begins to decrease; the strain at $\psi(\epsilon) = 0.95$ will be defined as the "critical buckling strain." If the foam exhibits a flat plateau in the load–compression curve, this is reflected as a slope of -1.0 in the log $\psi(\epsilon)$–log ϵ curve: the smaller this negative slope, the less pronounced is the plateau in the load–compression curve. A negative slope greater than 1.0 reflects a maximum in the load–compression curve (sample L). At some characteristic degree of compression, $\psi(\epsilon)$ displays a minimum, representing the point at which no further collapse of the matrix is possible, followed by a rapid rise. When all of the voids have been compressed out of the matrix, $\epsilon \approx 1 - \varphi$, $\psi(\epsilon)$ becomes greater than unity. Therefore, $\psi(\epsilon)$ can be characterized in terms of four quantities: (1) the critical buckling strain, (2) the average negative slope, (3) the minimum value of $\psi(\epsilon)$, and (4) the strain at $\psi(\epsilon)_{min}$.

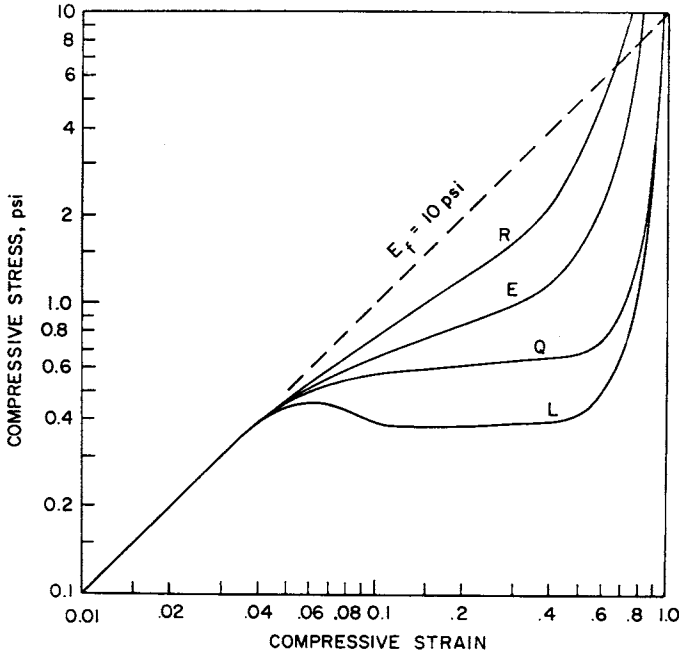

Fig. 3. Reduced compressive stress–strain curves for low-density, flexible foams of different cell geometry.

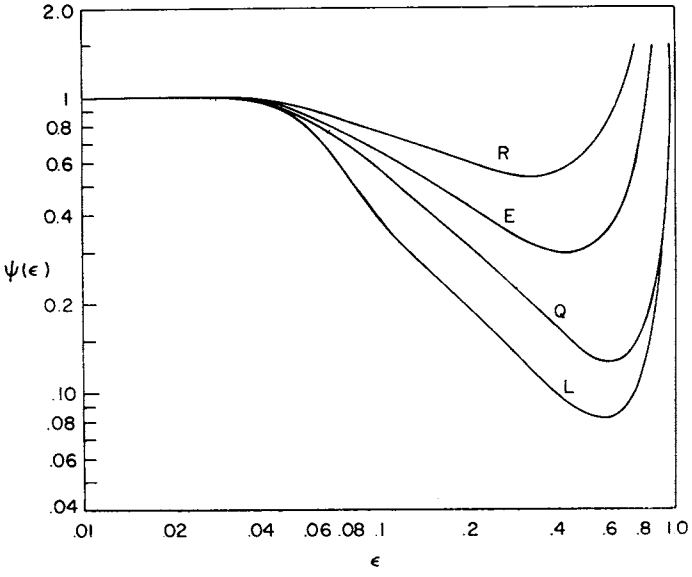

Fig. 4. The $\psi(\epsilon)$ functions calculated from the compressive stress–strain curves in Figures 2 and 3.

Ideally, $\psi(\epsilon)$ should be independent of the geometric shape of the foam test piece. But the lateral constraints of the matrix at large compressions, that is, the contribution to the compressive stress resulting from deformation (bulging) perpendicular to the applied stress, will be a function of the exterior dimensions. This is analogous to the uniaxial compression of a homogeneous rubber block, which has been described by Gent and Lindley.[9] The lateral constraints begin to contribute significantly to the compressive stress in the region of $\psi(\epsilon)_{\min}$, where the compressive stress no longer reflects primarily the buckling of the matrix, and are relatively more significant for high-density than low-density foams. This will be discussed in greater detail in a subsequent article.

In the present work, the bulk dimensions of all test pieces are similar, and the effect of the dimensions on $\psi(\epsilon)$ is not evaluated. Data were obtained, however, which indicate that $\psi(\epsilon)$ is independent of E_0 and strain rate but highly dependent on matrix geometry. The dependence of $\psi(\epsilon)$ on cell size, cell structure, and foam density is discussed in the following sections.

EXPERIMENTAL

Load–compression curves were obtained for a series of flexible polyurethane foams varying in cell-size from 0.012 to 0.10 in. and in density from $\varphi = 0.037$ to 0.34. The samples were obtained from Mobay Chemical Company and Scott Paper Company. The physical characteristics of these foams are summarized in Table I. The average cell size and the cell size range encompassing about 95% of the cells were estimated from a visual observation on photomicrographs of a known magnification.

Two types of polyurethane foams were examined: (1) normal polyurethane foam consisting of ribs of polymer outlining the individual cells with membranes, or cell walls, between some of the cells and (2) "reticulated" polyurethane foam, in which all of these cell walls have been removed by a thermal process. The differences in cell structure obtainable in low-density polyurethane foam are shown in Figure 5. A polyurethane foam with a highly regular cell structure and many cell walls is shown in Figure 5a; this will be denoted as type II. A similar foam with the cell walls removed by a reticulation process is shown in Figure 5b. A polyurethane foam with an irregular cell size and only a few cell walls (but not reticulated) is shown in Figure 5c; this "breadlike" structure will be denoted as type I.

For comparison, load–compression data also were obtained for a single sample of "latex" foam (Goodyear Tire and Rubber Company) (Table I). This type of foam is prepared by the frothing and subsequent coagulation and curing of a compounded rubber latex. A latex foam never contains cell walls. The cell structure of this foam is shown in Figure 5d.

The compression test pieces measured 2 × 4 × 4 in. and were compressed in the 2-in. direction. Ideally, the test piece thickness should be at least 50 times the average cell size to minimize the edge effect when computing

strain, but thicker samples of all the foams were not available. All the data presented were obtained at room temperature and at a strain rate of about 0.5%/sec, unless noted otherwise.

The load–compression behavior of polymeric foams is found to be elastically retarded, that is, a large hysteresis loop is observed; the hysteresis is substantially larger than that found in similar solid rubbery polymers. In addition, during the second compression the foam may exhibit an apparent stiffness which is lower than that during the first compression. The data

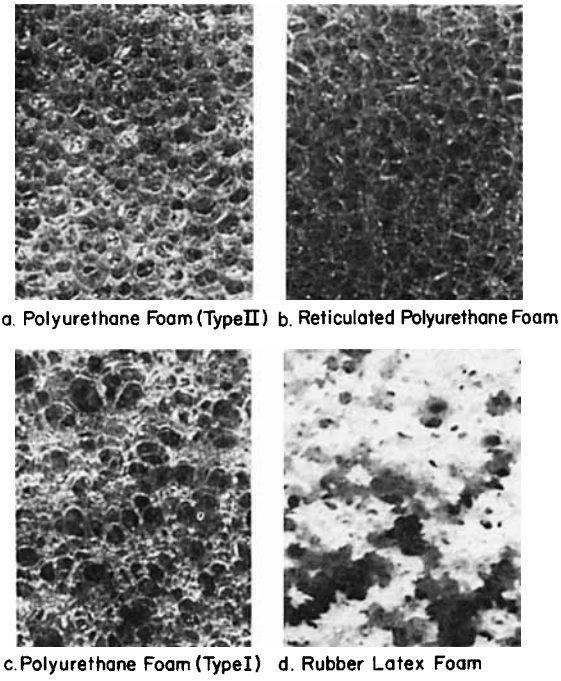

Fig. 5. Photomicrographs showing the differences in cell geometry obtained in low-density foams.

reported here represent an increasing compressive load and are characteristic of the first compression only, unless a specific reference is made to a second or third compression cycle.

To measure the modulus of the foam in tension and to check linearity of the load–deformation curve through $\epsilon = 0$, foam blocks (2 × 2 × 4 in.) were bonded between aluminum plates with an epoxy-type adhesive and extended, or compressed, in the 4-in. direction. In all cases, the curves were essentially linear from $\epsilon = -0.02$ to $+0.02$ (positive strain represents compression). The data for E_f are listed in Table I.

RESULTS AND DISCUSSION

Temperature and Strain Rate Dependence of $\Psi(\epsilon)$

To evaluate its temperature dependence, $\psi(\epsilon)$ was calculated from load–compression data obtained at 25, 60, and 100°C for foam samples C, E, G, H, N, and P. Increasing the temperature decreases E_0, and hence E_f, but does not alter the geometric structure of the matrix. The temperature dependence of E_f is given in Table II. In all cases, although E_f is decreased by a factor of about 1.5 to 2.5, $\psi(\epsilon)$ for a given sample is found to be independent of temperature, and hence independent of E_0. If, however, the change in temperatures causes the matrix to become brittle or to degrade, $\psi(\epsilon)$ does change. Small changes in $\psi(\epsilon)$ for these polyurethane foams are observed at −60°C; and at −196°C, large changes in $\psi(\epsilon)$ are observed. These changes in $\psi(\epsilon)$ are attributed to brittleness of the matrix at low temperatures. The differences between rigid and flexible foams will be discussed in greater detail in a subsequent article.

TABLE II
Effect of Temperature on E_f

Sample	E_f, psi		
	25°C	60°C	100°C
C	25.	18.	12.
E	4.5	2.8	1.7
G	15.	13.5	12.
H	9.0	7.7	5.8
N	9.4	7.1	5.8
P	16.	13.	10.

The strain rate dependence of $\psi(\epsilon)$ was evaluated from load–compression data for foam samples F, J, M and Q; and $\psi(\epsilon)$ was observed to be independent of strain rate over the range of 0.1% to 20%/sec. At 25°C, E_f is not changed appreciably by variations in strain rate.

Density Dependence of $\Psi(\epsilon)$

The effect of the volume fraction of polymer, φ, on $\psi(\epsilon)$ for foams of similar cell geometry is shown in Figure 6 for type I polyurethane foams (φ = 0.037 to 0.34) and in Figure 7 for type II polyurethane foams (φ = 0.033 to 0.105). In general, increasing φ increases $\psi(\epsilon)_{\min}$ and the critical buckling strain ϵ_b. From the data in Figures 6 and 7 the following proportionality can be written:

$$\psi(\epsilon)_{\min} \propto \varphi^{0.28}. \tag{3}$$

This relation is empirical and cannot be expected to hold for all types of foams. The function $\psi(\epsilon)$ is highly sensitive to cell geometry, and changing

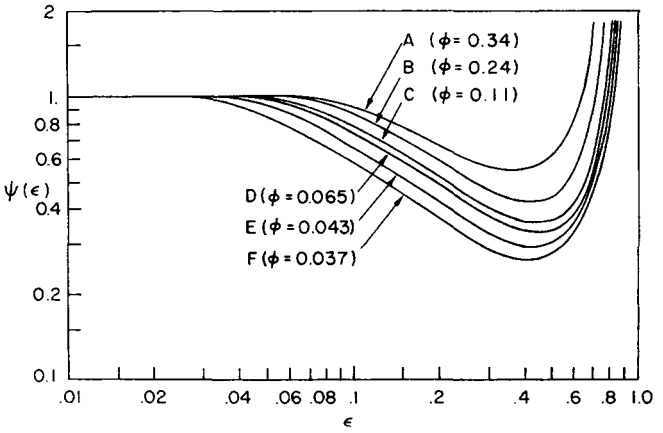

Fig. 6. The dependence of $\psi(\epsilon)$ on volume fraction of polymer for type I polyurethane foams.

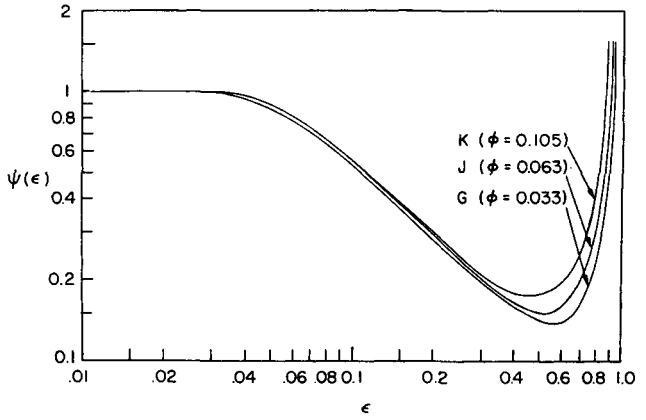

Fig. 7. The dependence of $\psi(\epsilon)$ on volume fraction of polymer for type II polyurethane foams.

the foam density may result in geometric changes which will cause $\psi(\epsilon)_{\min}$ to vary in a different manner than that given by eq. (3).

From eq. (2) it can be seen that E_f is strongly dependent on φ. Thus, for foams of similar geometry, the primary effect of density on the overall load–compression curve is the change in E_f. Changes in $\psi(\epsilon)$ may be of secondary importance; for example, taking a foam with $\varphi = 0.03$, the increase in φ required to double $\psi(\epsilon)_{\min}$ would cause E_f to increase by a factor of about 40. Additionally, the load-bearing capacity of a flexible foam is commonly expressed as the stress at 10% or 25% compression. In this region the changes in $\psi(\epsilon)$ may be much less than those in the region of $\psi(\epsilon)_{\min}$ (Fig. 7), and the load-bearing capacity will be closely proportional to E_f.

Cell Size Dependence of $\Psi(\epsilon)$

The effect of cell size on $\psi(\epsilon)$ for a series of reticulated polyurethane foams of similar density is shown in Figure 8. With the exception of sample N, the general effect of decreasing average cell size, d, is to increase $\psi(\epsilon)_{min}$:

$$\psi(\epsilon)_{min} \propto d^{-0.2}. \tag{4}$$

The value of ϵ_b does not appear to depend significantly on d, but the slope of the log $\psi(\epsilon)$–log ϵ curve in the region of 8% compression is dependent on d. Samples M and L exhibit a negative slope greater than 1.0, reflecting a maximum in the load–compression curve at about 6% compression (Fig. 2).

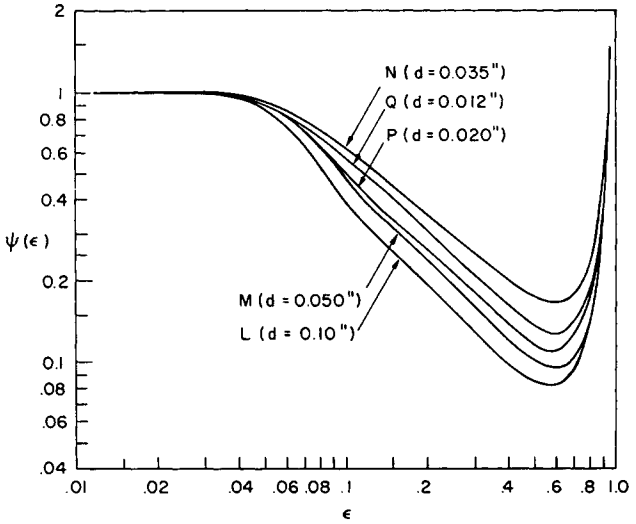

Fig. 8. The dependence of $\psi(\epsilon)$ on average cell size for reticulated type II polyurethane foams.

The $\psi(\epsilon)$ function is highly dependent on the geometric structure of the matrix; but this geometry is not adequately described in terms of an average cell size. This undoubtedly accounts for the relative position of the $\psi(\epsilon)$ curve for sample N in Figure 8; this foam had a noticeably less regular cell structure than the other reticulated foam samples. Therefore, while $\psi(\epsilon)$ is dependent on d, other geometric features of the matrix may be much more significant.

Structural Dependence of $\psi(\epsilon)$

To assess the dependence of $\psi(\epsilon)$ on the geometric structure of the matrix, $\psi(\epsilon)$ was calculated for several foams of similar density (φ = 0.03–0.04) but widely different cell geometry. This comparison is shown in Figure 9. Samples G and H (broken lines) are normal polyurethane foams

with a regular cell-structure (type II); samples Q and P are foams of similar cell size and structure after reticulation. For both types of polyurethane foams, $\psi(\epsilon)_{min}$ increases as d decreases, but the effect of the removal of cell walls on $\psi(\epsilon)$ is greater than the effect of doubling the average cell size. An additional comparison is provided with sample E; this polyurethane foam has a φ and d similar to that of samples G and P, but it has a highly irregular cell structure (type I). Thus, as the cell structure becomes more regular, or cell walls are removed, $\psi(\epsilon)_{min}$ decreases and the negative slope increases; ϵ_b does not appear to be significantly changed by the cell structure. The large effect of structure on $\psi(\epsilon)$ also is demonstrated in Figure 4. A rubber latex foam (sample R) has a highly irregular cell structure, which accounts for the relatively low negative slope (reflecting a less pronounced plateau in the load–compression curve) and high $\psi(\epsilon)_{min}$.

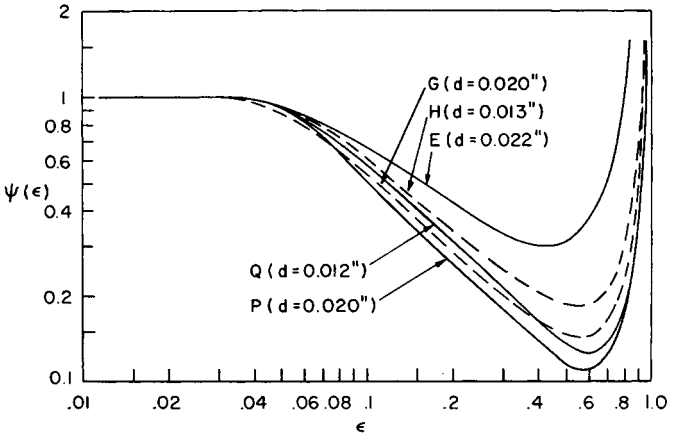

Fig. 9. The dependence of $\psi(\epsilon)$ on cell geometry for foams of similar density.

Because of differences in matrix geometry, a polyurethane foam may possess the same apparent Young's modulus as a latex foam but only 30% of the load-bearing capacity at 25% compression and only 15% at 50% compression.

The data in Figures 4 and 9 clearly show that $\psi(\epsilon)$ is influenced most strongly by the specific details of the matrix geometry and that the volume fraction of polymer and average cell size are of secondary importance only. Unfortunately, this geometric character is a difficult quantity to describe quantitatively and it can be defined only in terms of a comparison to a matrix of known geometry.

It is important to note that E_f/E_0 is rather insensitive to the details of the matrix geometry and depends primarily on φ. Therefore, when designing a foam for a particular application, if the *shape* of the load–compression curve is unacceptable, the cell geometry must be altered. On the other hand, if the shape is acceptable but the stiffness is not, then the density or E_0 must be altered. In addition, temperature and strain rate changes influ-

ence primarily E_0 such that the shape of the load–compression curve tends to be independent of these variables.

Fatigue of Polyurethane Foams

The load–compression curve of a polyurethane foam is sensitive to the previous compression history of the foam, exhibiting a decreasing stiffness and load-bearing capacity with an increasing number of compression cycles. Both E_f and $\psi(\epsilon)$ are observed to change; however, the relative decrease is largest during the first and second compression cycles. For polyurethane foams C, G, K, and M, the effect of compression history on E_f is listed in

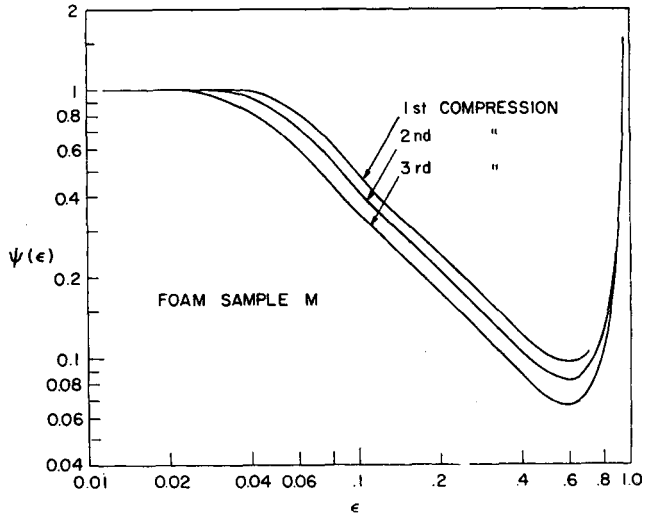

Fig. 10. The dependence of $\psi(\epsilon)$ on compression history for a typical reticulated polyurethane foam.

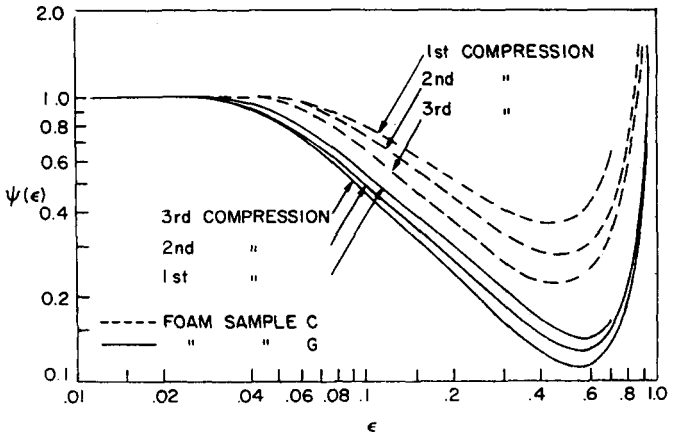

Fig. 11. The dependence of $\psi(\epsilon)$ on compression history for typical polyurethane foams.

TABLE III
Effect of Compression on E_f

Sample	E_f, psi		
	1st Comp.	2nd Comp.	3rd Comp.
C	25.0	24.5	24.0
G	15.0	13.2	12.5
K	32.0	31.5	29.0
M	14.0	13.7	13.2

Table III, and the effect on $\psi(\epsilon)$ is shown in Figures 10 to 12. A fourth compression cycle displayed only negligible changes in either E_f or $\psi(\epsilon)$ from the third cycle. The degree of compression was about 70% during the first cycle and about 95% during the second, third, and fourth cycles. The loss in stiffness and load-bearing capacity is attributed to tearing of the foam matrix, and thus the relative changes in E_f and $\psi(\epsilon)$ would be less if the degree of compression were less severe.

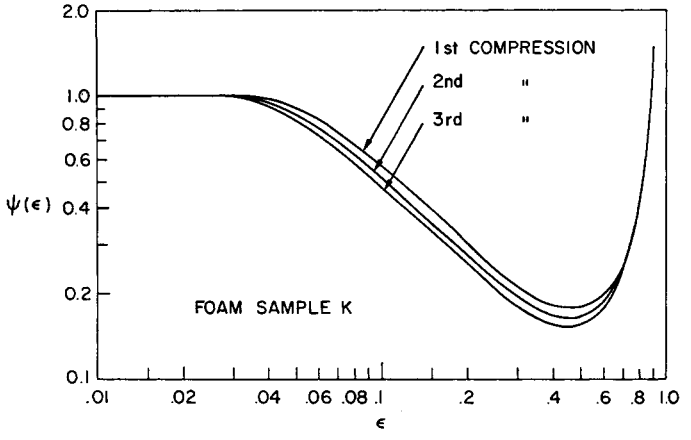

Fig. 12. The dependence of $\psi(\epsilon)$ on compression history for a typical type II polyurethane foam.

The general effect of previous compression cycles on $\psi(\epsilon)$ is to decrease $\psi(\epsilon)_{\min}$ and ϵ_b. For samples C and G there also is a noticeable increase in the negative slope of the $\psi(\epsilon)$ function, denoting a more pronounced plateau in the load–compression curve. The identical compression history produced slightly different relative changes in $\psi(\epsilon)$ for each polyurethane foam, but the present data do not suggest any specific relationship between these changes in $\psi(\epsilon)$, that is, the fatigue resistance and the geometric structure of the foam.

It is interesting to note that rubber latex foams exhibit a high degree of fatigue resistance compared to polyurethane foams. For foam sample R, four compression cycles (70% compression) produced no detectable changes

in E_f or $\psi(\epsilon)$. The reason for this difference is uncertain, but it may result from the fact that the latex foam matrix is partially torn during the manufacturing process such that no additional tearing takes place during compression.

APPLICATIONS OF LOAD–COMPRESSION RELATIONS

From a knowledge of $\psi(\epsilon)$ and E_f and their dependences on foam parameters—density, cell shape and size distribution, and modulus of the base polymer—it is possible to delineate precisely the physical characteristics a foam must possess to meet a given load–compression specification. The optimum type of foam for a particular application now can be determined with a minimum of trial-and-error evaluation. For example, if the shape of the load–compression curve is not suitable for a given application, then the cell geometry of the foam must be altered to achieve the desired $\psi(\epsilon)$; but if the shape is satisfactory while the stiffness is not, then the volume fraction of polymer or the modulus of the matrix polymer must be altered to achieve the desired E_f (eq. 2).

Additionally, a knowledge of the dependence of $\psi(\epsilon)$ on matrix geometry makes it possible to estimate the shape of the entire load–compression curve from a limited amount of experimental data. For example, frequently the compressive stress is known at a single compressive strain only, such as $\epsilon = 0.25$. Knowing E_f, $\psi(\epsilon)$ can be calculated at this strain (eq. 1); and from a knowledge of the general type of cell structure, the load–compression curve can be estimated over the entire range of compressive strain which is of interest. If experimental data for E_f are not available, E_f can be estimated from the foam density and physical properties of the matrix polymer (eq. 2).

Generally the temperature and rate dependence of the modulus are known for the base polymer but not for the foam. Since $\psi(\epsilon)$ is essentially independent of temperature or strain rate and E_f is directly proportional to E_0, the modulus of the base polymer, the temperature and rate dependence of the compression curve for a given foam can be calculated from that of E_0. This is particularly valuable when a knowledge of the load–compression curve is required at a particular temperature and rate which cannot be achieved with the available experimental facilities.

CONCLUSIONS

The compressive stress characteristics of a foam can be factored into the product of (1) a dimensionless function of compressive strain, $\psi(\epsilon)$, reflecting the buckling of the matrix, and (2) a factor ϵE_f, where ϵ is the compressive strain and E_f the apparent Young's modulus of the foam. E_f is a function primarily of Young's modulus of the matrix polymer, E_0, and of the volume fraction of polymer; while $\psi(\epsilon)$ is highly sensitive to the specific details of the matrix geometry, only moderately dependent on density or cell size, and independent of E_0 (and hence independent of temperature or

strain rate). The experimentally evaluated strain function, $\psi(\epsilon)$, cannot be expressed exactly by any simple analytical expression; but the critical features of $\psi(\epsilon)$, plotted on logarithmic coordinates, are shown to vary in a regular and predictable manner with changes in the matrix geometry.

It is a pleasure to acknowledge Drs. W. J. Burlant and S. Newman for their support during the course of this work and Mr. R. E. Goeboro for performing the experimental measurements.

References

1. E. Guth, P. E. Wack, and R. L. Anthony, *J. Appl. Phys.*, **17**, 347 (1946).
2. T. L. Smith, *Trans. Soc. Rheol.*, **6**, 61 (1962).
3. A. N. Gent and A. G. Thomas, *J. Appl. Polym. Sci.*, **1**, 107 (1959); *Rubber Chem. Technol.*, **36**, 597 (1963).
4. J. D. Griffin and R. E. Skochdopole, in *Engineering Design for Plastics* (E. Baer, ed.), Reinhold, New York, 1964, p. 995.
5. T. H. Ferrigno, *Rigid Plastics Foams*, 2nd Edition, Reinhold, New York, 1967.
6. E. H. Kerner, *Proc. Phys. Soc.* (London), **B69**, 808 (1956).
7. J. K. Mackenzie, *Proc. Phys. Soc.* (London), **B63**, 2 (1950).
8. K. C. Rusch, unpublished data.
9. A. N. Gent and P. B. Lindley, *Proc. Instn. Mech. Eng.*, **173**, 111 (1959).

Received March 21, 1969
Revised May 9, 1969